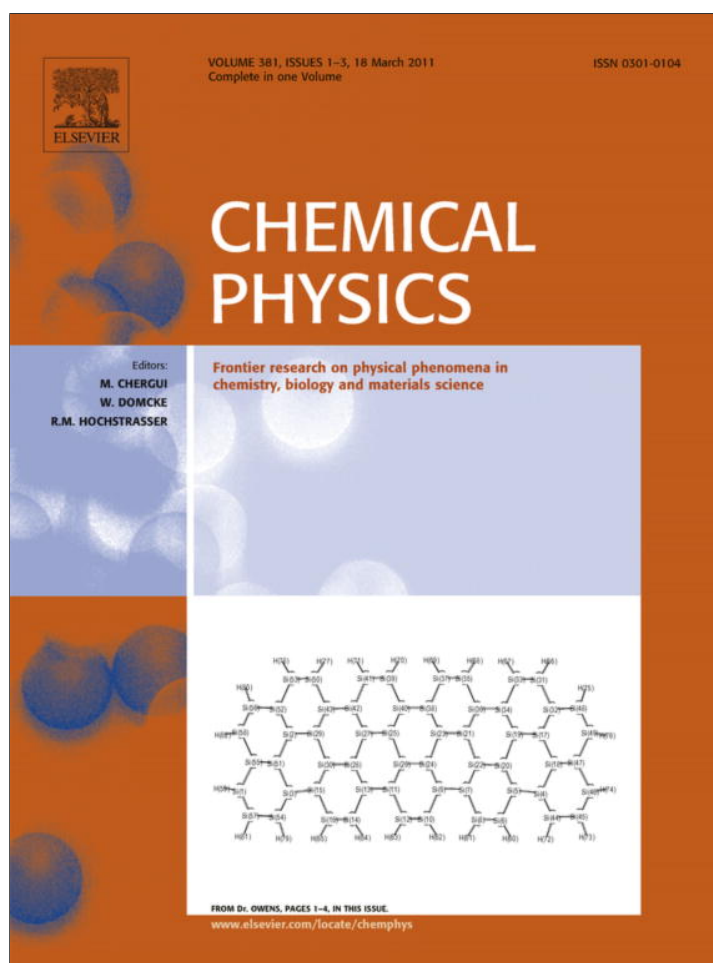


Provided for non-commercial research and education use.
Not for reproduction, distribution or commercial use.



This article appeared in a journal published by Elsevier. The attached copy is furnished to the author for internal non-commercial research and education use, including for instruction at the authors institution and sharing with colleagues.

Other uses, including reproduction and distribution, or selling or licensing copies, or posting to personal, institutional or third party websites are prohibited.

In most cases authors are permitted to post their version of the article (e.g. in Word or Tex form) to their personal website or institutional repository. Authors requiring further information regarding Elsevier's archiving and manuscript policies are encouraged to visit:

<http://www.elsevier.com/copyright>



Size dependence and effect of potential parameters on properties of nano-cavities in liquid xenon using molecular dynamics simulation

Hamed Akbarzadeh^{a,*}, Hadi Abroshan^a, Farid Taherkhani^b, Cobra Izanloo^a, Gholam Abbas Parsafar^{a,*}

^aDepartment of Chemistry and Nanotechnology Research Center, Sharif University of Technology, Tehran, 11365-9516, Iran

^bDepartment of Chemistry, Science College, Razi University, Kermanshah, Iran

ARTICLE INFO

Article history:

Received 27 July 2010

In final form 13 January 2011

Available online 20 January 2011

Keywords:

Molecular-dynamics

Lennard–Jones liquid

Nano-cavity

ABSTRACT

We have investigated the size dependence of a nano-cavity properties produced in a Xe fluid using molecular dynamics simulations. We have created a nano-cavity of different sizes at 170 and 200 K (cavities diameters are within 1–10 nm). Liquid pressure, vapor pressure and surface tension of the nano-cavity for some given values of diameter are calculated. Within 1–10 nm cavity diameter, we have observed two opposite behavior for dependency of surface tension on the cavity diameter: for the range of 1–5 nm, it increases with the diameter, while, for the range of 5–10 nm remains constant. Also, the value of liquid pressure becomes less negative, when the size of cavity increases. Vapor pressure in the cavity was found to be independent of cavity size.

In this paper, we have also studied the effects of Lennard–Jones potential parameters on the surface tension (while temperature and cavity radius are held constant).

© 2011 Elsevier B.V. All rights reserved.

1. Introduction

Nanoscience and nanomaterials have been identified world widely as the key to unlocking a new generation of devices with revolutionary properties and functionalities [1].

Cavitation is one of the fundamental phenomena in fluid mechanics. This phenomenon is often observed in pumps, orifice, venture tube, liquid jet where high-speed liquid flows occur, and is also observed in fluids in an acoustic field. Although cavitation has many negative aspects such as decline of performance and vibration in pumps, erosion on a solid surface and noise. Recent studies suggest that this phenomenon can also provide valuable applications for cleaning and medical purposes. Now a better understanding and the control of the cavitations process are strongly required, and they will enable us to design more reliable fluid machinery and to develop new techniques [2]. Micro-cavities have recently gained much attention in many fields. In particular, cavities with size of sub-micrometer, or “nano-cavity”, have become an attractive research target, partly because of recent technological progress of micro-cavity generations and partly in prospect of their fruitful applications, such as sensors and optical treatments. However, experimental investigation of their physical properties is far behind the applications due to their size and fragileness [3]. For example, controlling the cavitation process is related to

designing a high-performance ship propeller. From scientific point of view, the cavitation is understood as a typical example of nucleation processes, and is related to thermodynamic properties and the limit of metastable liquid. From a microscopic viewpoint, despite this importance, less attention has been paid to cavitation and properties of liquid under negative pressure [4]. Recently, many works have done in this area [4–10].

In 2008, Matsumoto et al. investigated size dependence of surface tension nano-bubble in argon liquid. They showed that surface tension evaluated with assumption of the Young–Laplace (Y–L) equation has minor dependence on the bubble radius, and agrees with the surface tension of a planer interface [3]. The Y–L equation describes the difference between inside pressure and outside pressure of a spherical cavity due to the surface tension. The Y–L equation is simply deduced from mechanical stability of a cavity. The pressure difference inversely increases with the cavity radius. The Y–L equation is [11,12]:

$$P_{\text{vap}} = P_{\text{liq}} + \frac{2\gamma}{R} \quad (1)$$

where P_{vap} and P_{liq} are the pressure inside (vapor phase) and outside (liquid phase) of the cavity, respectively, γ is the surface tension, and R is the cavity radius. Comprehensive studies of the cavity, bubble, and droplet, have been carried out over the past decades [3,13–22].

We have carried out molecular dynamics simulation to obtain both P_{liq} and P_{vap} for a nano cavity with various sizes. Then by assuming Eq. (1), we have calculated the surface tension and investigated its size dependence. Also we have studied effects of

* Corresponding authors. Tel.: +98 21 66165355, fax: +98 21 66005718.

E-mail addresses: akbarzadehhamed@yahoo.com (H. Akbarzadeh), parsafar@sharif.edu (G.A. Parsafar).

Table 1

Calculated number density of liquid in the nano-cavity at $T = 170$ K and $T = 200$ K temperatures, when the total number of xenon atoms is 32,000. Percent deviation of the cavity diameter is given in parenthesis.

Temperature (K)	Cavity diameter (nm)	Number density of liquid (nm^{-3})
170	1 (−3.30)	12.578
170	2 (+3.38)	12.876
170	3 (−3.09)	13.058
170	4 (−2.75)	13.174
170	5 (+1.02)	13.290
170	6 (+1.32)	13.389
170	7 (−1.57)	13.439
170	8 (+1.35)	13.463
170	9 (+1.00)	13.480
170	10 (+0.70)	13.492
200	1 (−1.94)	9.946
200	2 (−2.56)	10.244
200	3 (+1.31)	10.426
200	4 (−2.30)	10.575
200	5 (−1.60)	10.658
200	6 (−2.01)	10.741
200	7 (+1.08)	10.807
200	8 (+1.41)	10.857
200	9 (−1.28)	10.890
200	10 (−1.01)	10.915

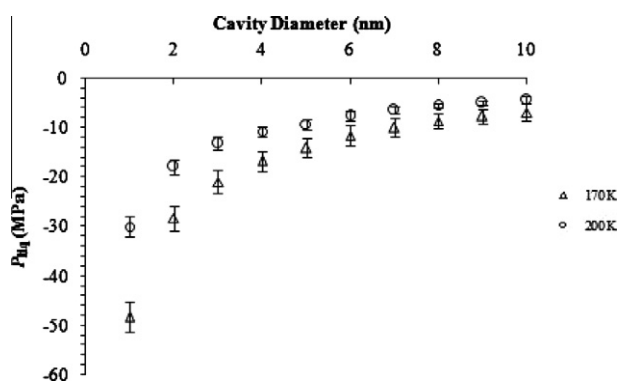


Fig. 1. Dependency of the liquid phase pressure on the cavity size (at $T = 170$ and 200 K) with the same number of particles ($N = 32,000$).

Lennard–Jones potential parameters (ϵ , σ) on the liquid pressure, vapor pressure and surface tension.

2. Molecular dynamics simulation

In this paper, the procedure used is similar to that introduced in references [3,4].

In the present study, molecular dynamics simulation on the bulk of liquid Xe was done using the DL-POLY-2.20 program [23]. Xenon particles are confined in a cubic cell with the three-dimensional periodic boundary conditions. We have performed the simulation on a FCC lattice of Xe atoms with LJ (12–6) parameters, $\sigma = 3.924$ Å and $\epsilon = 2.1383$ (kJ/mol) [24].

$$V_{LJ}(r) = 4\epsilon \left[\left(\frac{\sigma}{r} \right)^{12} - \left(\frac{\sigma}{r} \right)^6 \right] \quad (2)$$

The MD simulations are carried out in a NVT ensemble with a constant number of atoms N , volume V , and temperature T with the periodic boundary conditions. Xenon lattice has a FCC structure. A FCC block was first constructed from a FCC unit cell by replication in three dimensions with the center located at $(0, 0, 0)$. The fractional coordinates in the FCC structure are $(0, 0, 0)$, $(0.5, 0.5, 0)$, $(0.5, 0, 0.5)$, and $(0, 0.5, 0.5)$. Temperature is controlled by a Nose–Hoover thermostat [25] and the equations of motion are integrated

using the Verlet Leapfrog algorithm [26] with a time step of 0.001 ps. The system was equilibrated for 500 ps (500,000 time steps), the averages were computed over the next following 1 ns (10,00,000 time steps). The cutoff length is chosen to be 9 Å in the simulations. In these systems, the number of particles is $N = 32,000$. (To test that the system is equilibrated, we have plotted thermodynamic quantities such as potential energy and temperature as a function of time. When equilibrium is reached: the quantities should fluctuate around the average values and the averages should remain constant with time (no systematic drift).)

First, the system was equilibrated at a chosen temperature T with volume V corresponds to a normal liquid state (liquid without any cavities with pressure close to zero at the given temperature). Then, a spherical repulsive external force field has been applied at the central part of the cell to generate a tiny cavity. After the equilibrium is reached, the force field is removed [3]. With varying the system volume V , we can obtain a liquid containing a single cavity with various sizes. In this work, we have investigated the system at two different temperatures, namely 170 K and 200 K. (Xenon at these temperatures is in the liquid state, at ordinary pressures). Also, we have changed the Lennard–Jones parameters (ϵ , σ) in the force field file to investigate the effects of these parameters on liquid pressure, vapor pressure, and surface tension.

Several particles, which have been evaporated spontaneously, are inside the cavity.

The result for number density of the liquid for various cavity diameters at 170 K and 200 K is summarized in Table 1.

3. Results

In this study, the liquid pressure is calculated via the usual virial expression.

Pressure evaluated for the whole system was found to be almost equal to P_{liq} because the contribution of the cavity region is much smaller than that of the liquid region. The results are shown in Fig. 1.

The fact that creating a cavity inside a liquid requires transferring some molecules from the bulk to the surface, for which potential energy increases; therefore, some work has to be done. Such increase in the potential energy leads to a negative force and hence negative pressure. Transfer of a molecule from a large cavity surface to the liquid surface needs less work, compared to a small cavity. For instance, if surface of the cavity is large enough no significant work needed to transfer some molecules from its surface to the liquid surface. Therefore, we may expect that liquid pressure becomes a less negative value, when the size of cavity increases, as shown in Fig. 1. At lower temperatures, at which the liquid cohesive energy is more (stronger attraction among the molecules), we may expect that the transfer of a molecule from the cavity surface to the liquid surface requires more reversible work; as a result, the liquid pressure becomes a larger negative number, as shown in Fig. 1.

For calculation of vapor pressure (P_{vap}), we have used the empirical equation of state for gaseous Xe [27]:

$$P = k_{11}T\rho + (k_{02} + k_{12}T + k_{22}T^2)\rho^2 + (k_{03} + k_{13}T + k_{23}T^2)\rho^3 + k_{04}\rho^4 + k_{05}\rho^5 \quad (3)$$

where values of k_{ij} parameters are given in Table 2. The values are based upon the use of a coherent system of SI units (MPa for pressure, kg/L for density, K for temperature).

We have directly calculated ρ_{vap} by simply counting number of particles inside the cavity and dividing it to the cavity volume. By evaluating ρ_{vap} of the cavity and using the equation of state, P_{vap} can be calculated. The results are shown in Fig. 2 for the two isotherms.

Table 2
The values of parameters of empirical equation of state for gaseous xenon [27]. Note that the SI units are used (MPa for pressure, kg/L for density, K for temperature).

Substance	k_{11}	k_{02}	k_{12}	k_{22}	k_{03}	k_{13}	k_{23}	k_{04}	k_{05}
Xe	0.063328	-41.125	0.09280	-0.0000546	12.413	-0.04145	0.0000443	3.921	-1.748

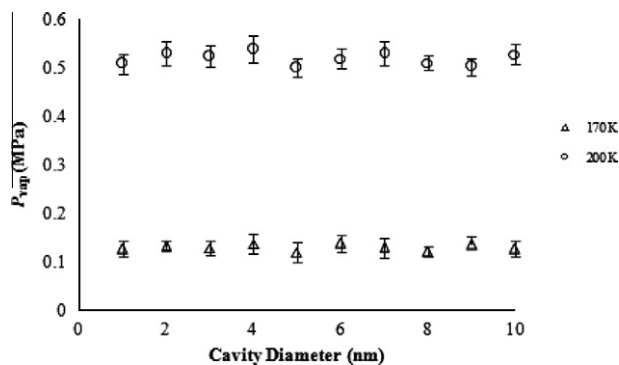


Fig. 2. Dependency of the vapor pressure inside cavity to the cavity size with the same number of particles ($N = 32,000$) at 170 K and 200 K.

P_{vap} at $R \rightarrow \infty$ is the vapor pressure for the flat surface, more specifically the saturated vapor pressure of the liquid, which was obtained from the MD simulations for a flat liquid layer (0.1301 MPa at $T = 170$ K, and 0.5183 MPa at $T = 200$ K). The experimental saturated vapor pressure of the liquid bulk at 170 K and 200 K are 0.13343 MPa and 0.52091 MPa, respectively [26]. It is interesting that the calculated P_{vap} is almost independent of the cavity size and is nearby the bulk value. Since the cavity surface is considered as a rigid wall for the gas in the nanocavity, such a result is expected. We may also give a reason for such a behavior on the basis of thermodynamic arguments as follows: since at equilibrium there is no net mass transfer between the liquid bulk and cavity, we may conclude that the chemical potential of Xe in the bulk and cavity at temperature T are equal; therefore,

$$\mu(P_{vap}) = \mu[P_{liq}, \rho_{liq}] \quad (4)$$

where $\mu(P_{vap})$ and $\mu[P_{liq}, \rho_{liq}]$ are the chemical potential of Xe in the cavity and liquid, respectively. Note that at constant temperature, P_{vap} depends on both P_{liq} and the surface tension. The negative liquid pressure, P_{liq} , and the surface tension have opposite influences on P_{vap} ; namely when R reduces the former expands the cavity while the latter contracts it. The net effect of these two opposite factors on P_{vap} is not known. However, on the basis of the calculated results shown in Fig. 2, they almost cancel each other out; hence, P_{vap} becomes almost independent of the bubble size.

Now that both P_{liq} and P_{vap} are known, we can estimate the surface tension γ , assuming the Y–L equation, Eq. (1).

Fig. 3 shows cavity size dependence of the surface tension; the value for $R \rightarrow \infty$ was directly obtained from a separate MD simulation for a flat surface (0.01701 N/m at $T = 170$ K and 0.01193 N/m at $T = 200$ K). Fig. 3 shows two different behavior: for the sizes of 1–5 nm of cavity diameter, surface tension increases with cavity diameter, while for 5–10 nm, it becomes independent of the cavity size. The experimental surface tension for the flat surface of bulk xenon at 170 K and 200 K are 0.017525(N/m) and 0.012083(N/m), respectively [28].

It is shown that for simple liquids the effective pair interaction potential, at a given temperature, depends only on the average nearest neighbor separation and coordination number [29]. If the cavity is not too small (cavity diameter larger than about 5 nm), one may assume that half of a sphere on the surface of cavity is within the cavity and the other half is in the liquid, as in the case of a flat interface, see Fig. 4.

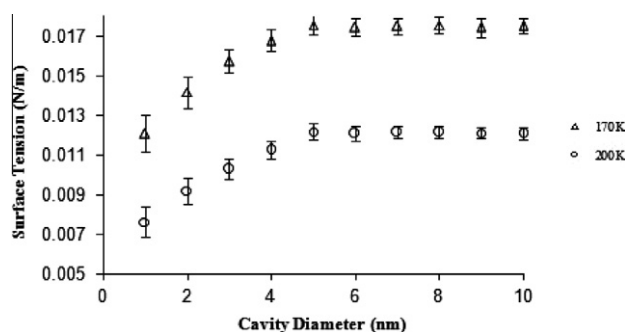


Fig. 3. Cavity size dependence of the surface tension. (at $T = 170$ and 200 K) for the same number of particles.

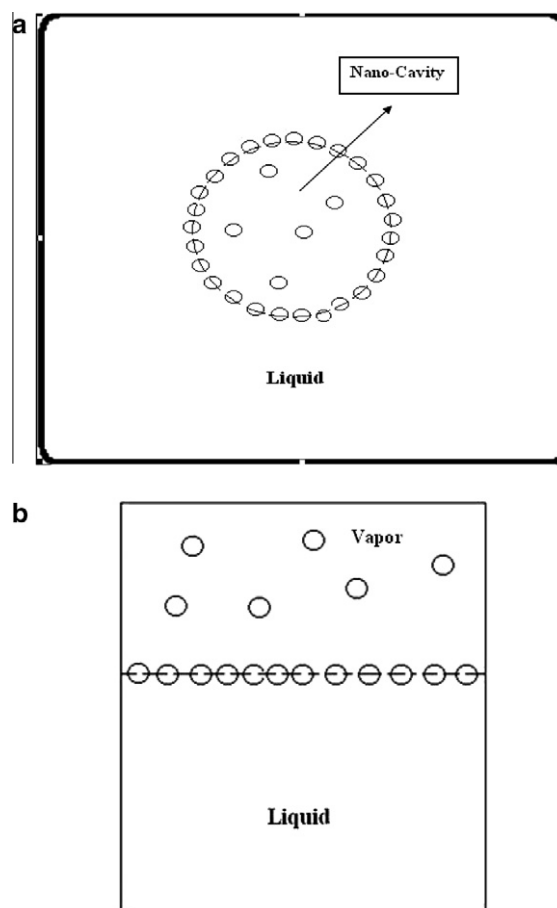


Fig. 4. Two-phase system of Xe shown in a two-dimensional space for (a) cavity and bulk liquid and (b) liquid and vapor. The interface is shown by a dashed line for each case. As shown, the number of nearest neighbors for a sphere on both interfaces with molecules in the liquid phase is almost the same, if the cavity is not too small.

Therefore, by assuming that the average molecular separation in the bulk and on the surface of liquid are the same, the reversible work needed to bring a molecule from the bulk to the cavity surface may be given as,

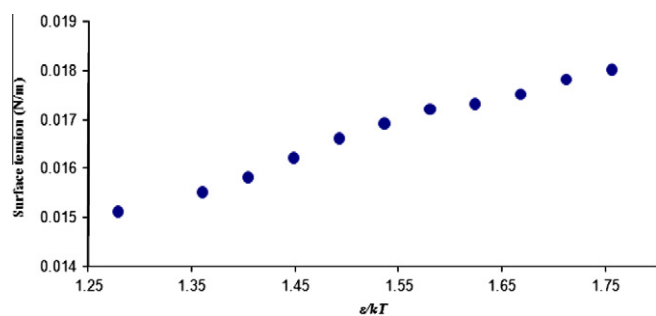


Fig. 5. Dependency of surface tension on the inverse of reduced temperature (ε/kT) at 170 K (Diameter = 10 nm, $\sigma = 3.924$ Å, $N = 32,000$).

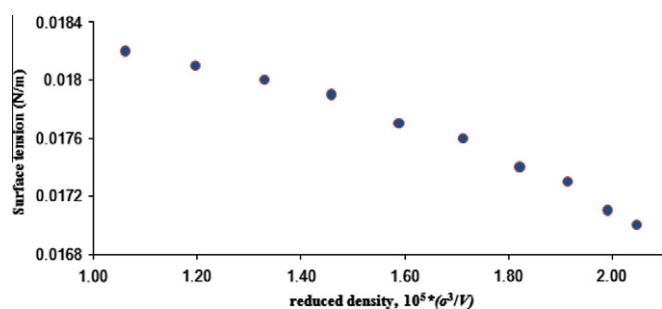


Fig. 6. Dependency of surface tension on the reduced density (σ^3/V) at 170 K, when Diameter = 10 nm and $\varepsilon = 2.1383$ kJ/mol.

$$W_{\text{rev}} = \left[\frac{Z^{\text{liq}}}{2} U^{\text{liq}} + \frac{Z^{\text{vap}}}{2} U^{\text{vap}} \right] - [Z^{\text{liq}} U^{\text{liq}}] = \frac{Z^{\text{vap}}}{2} U^{\text{vap}} - \frac{Z^{\text{liq}}}{2} U^{\text{liq}} \quad (5)$$

where Z^{vap} and Z^{liq} are the average number of nearest neighbors in the cavity and liquid (considering only the nearest neighbor interactions); and U^{vap} and U^{liq} are the average pair interaction energy in the cavity and liquid, respectively [30]. The U^{vap} and U^{liq} interaction energies are proportional to the vapor and liquid densities, respectively. Transfer of a molecule from the liquid to cavity surface will increase the surface by $1/2(4\pi r^2) = 2\pi r^2$, where r is the molecular radius. Therefore, surface tension (for the nanocavity-liquid interface) may be given as,

$$\gamma = \frac{W_{\text{rev}}}{2\pi r^2} = \frac{Z^{\text{vap}} U^{\text{vap}} - Z^{\text{liq}} U^{\text{liq}}}{4\pi r^2} \quad (6)$$

on the basis of Eq. (6), we may expect γ becomes independent of the cavity size (R) when the diameter is roughly larger than 5 nm, which is in accordance with our results given in Fig. 3. However, for cavity diameter less than 5 nm, surface tension increases with the cavity diameter, which is in agreement with the results of Tolman [19]. (Note that on the basis of Eq. (6), γ inversely varies with the square of molecular diameter.) The reason for such dependence is due to the fact that for large cavity curvature, the number of neighboring molecules within liquid for a molecule on the cavity surface depends on the cavity diameter.

3.1. Effect of potential parameters

Now, we may investigate the influence of the Lennard–Jones potential parameters (ε, σ) on physical properties of nanocavity. Firstly, we have changed ε within (1.806 kJ/mol)–(2.48 kJ/mol) via changing the reduced temperature (ε/kT) (at $T = 170$ K, when Diameter = 10 nm, $\sigma = 3.924$ Å). Therefore, Fig. 5 in fact shows the epsilon dependence of the surface tension. Increasing ε enhances the attraction energy between two molecules. Therefore,

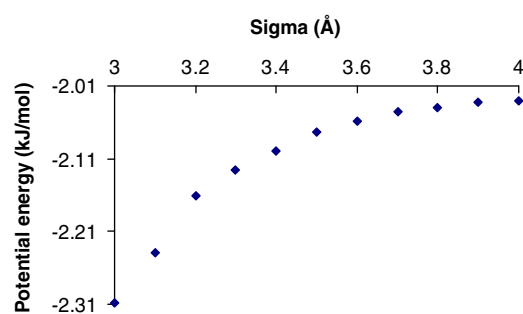


Fig. 7. The sigma dependence of potential energy at 170 K, when Diameter = 10 nm and $\varepsilon = 2.1383$ kJ/mol.

as Fig. 5 shows, γ increases with respect to ε (or the inverse of reduced temperature). This result is expected, because the energy needed to transfer a molecule from bulk to the surface of cavity will be more, when the attraction energy increases.

Also, we have changed the value of sigma within 3–4 Å via changing the reduced density (σ^3/V) [at $T = 170$ K, when Diameter = 10 nm, $\varepsilon = 2.1383$ kJ/mol]. Fig. 6 indeed shows sigma dependence of the surface tension.

Due to the fact that the increase of the LJ parameter sigma, on one hand, increases the repulsive hard-core size of the LJ particle and on the other hand increases the range of attraction, it is not straight forward to predict which contribution in the potential energy, repulsion or attraction, is dominating. In fact it can be shown that its impact on the second virial coefficient changes at the Boyle temperature. For this reason we have calculated the effective interaction potential for different values of sigma when $T, \varepsilon,$ and R are held constant. The results are depicted in Fig. 7. As shown in this Figure, for the range of investigation, $\sigma = 3\text{--}4$ Å, the net effect of increment of σ is to increase the potential energy, which means that the contribution of the repulsion term is dominating when σ increases. Therefore, one may expect that the effect of increase of σ on the surface tension is opposite to that of ε , see Figs. 5 and 6, at least for the range of investigation.

4. Conclusions

Using MD simulation with the Lennard–Jones (12–6) potential for liquid xenon, we have studied the size dependence of vapor nano-cavity properties. We have found that the vapor pressure inside the cavity is independent of the cavity radius, and is equal to the saturated vapor pressure of the liquid. When cavity becomes smaller, the molecules on its surface have higher potential energy; hence the liquid pressure is more negative. The surface tension is evaluated with the assumption of the Y–L equation which is also independent of the cavity radius, almost same as that of a flat interface, when the cavity radius is larger than ≈ 2.5 nm. However, it is shown that if the cavity radius is too small, namely smaller than about 2.5 nm, surface tension significantly increases with the radius. In such a case the number of nearest neighbors of a surface molecule with molecules within the liquid phase remarkably depends on the cavity radius. The value of epsilon (ε) is changed at constant temperature while the cavity radius and sigma (σ) are held constant. Increasing ε enhances the attraction among molecules; as a result, γ increases. Unlike the effect of ε on γ , the increase of σ within the range of investigation, 3–4 Å, resulted in decreasing of γ [Fig. 6], since the net effect of increment of σ is to reduce the interaction potential (Fig. 7).

References

- [1] T.E. Karakasidis, C.A. Charitidis, Mater. Sci. Eng. C 27 (2007) 1082.

- [2] S. Tsuda, S. Takagi, Y. Matsumoto, *Fluid Dynam. Res.* 40 (2008) 606.
- [3] M. Matsumoto, K. Tanaka, *Fluid Dynam. Res.* 40 (2008) 546.
- [4] T. Kinjo, M. Matsumoto, *Fluid Phase Equilib.* 144 (1998) 343.
- [5] K. Neyts, *Appl. Surf. Sci.* 244 (2005).
- [6] L. Zhang, X. Zhang, C. Fan, Y. Zhang, J. Hu, *Langmuir* 25 (2009) 8860.
- [7] W.A. Ducker, *Langmuir* 25 (2009) 8907.
- [8] Y. Wang, B. Bhushan, X. Zhao, *Langmuir* 25 (2009) 9328.
- [9] S. Yang, P. Tsai, E.S. Kooij, A. Prosperetti, H.J.W. Zandvliet, D. Lohse, *Langmuir* 25 (2009) 1466.
- [10] M.P. Brenner, D. Lohse, *Phys. Rev. Lett.* 101 (2008) 214505.
- [11] T. Young, *Philos. Trans. Roy. Soc. London* 95 (1805) 65.
- [12] P.S. Laplace, *Traite de Mechanique Celeste*, vol. 4, Gauthier-Villars, Paris, 1805.
- [13] J.W. Gibbs, *The Collected Works of J. W. Gibbs*, vol. 1, Longmans, New York, 1928, pp. 315.
- [14] L.G. Zhou, H.C. Huang, *Appl. Phys. Lett.* 84 (2004) 1940.
- [15] C.E. Brennen, *Cavitation and Bubble Dynamic*, Oxford University Press, Oxford, 1995.
- [16] V.P. Skripov, *Metastable Liquids*, Wiley, New York, 1974.
- [17] K. Koga, X.C. Zeng, A.K. Shchekin, *J. Chem. Phys.* 109 (1998) 4063.
- [18] H. Yaguchi, T. Yano, S. Fujikawa, in: *Proceedings of the International Conference on Multiphase Flow*, S4-Thu-D-59, 2007.
- [19] R.C. Tolman, *J. Chem. Phys.* 17 (1949) 333.
- [20] S.M. Thompson, K.E. Gubbins, J.P.R.B. Walton, R.A.R. Chantry, J.S. Rowlinson, *J. Chem. Phys.* 81 (1984) 530.
- [21] G. Nagayama, T. Tsuruta, P. Cheng, *Int. J. Heat Mass Transfer* 49 (2006) 4437.
- [22] S.H. Park, J.G. Weng, C.L. Tien, *Int. J. Heat Mass Transfer* 44 (2001) 1849.
- [23] W. Smith, I.T. Todorov, *Mol. Simulat.* 32 (2006) 935.
- [24] D.A. McQuarrie, *Statistical Mechanics*, vol. 236, University Science Books, 2000.
- [25] S. Nose, *J. Phys.: Condens. Matter* 2 (1990) 115.
- [26] M.P. Allen, D.J. Tildesley, *Simulation of Liquids*, Oxford University Press, London, 1987.
- [27] R. Sandri, *The Canadian J. Chem. Eng.* 65 (1986) 517.
- [28] <<http://Webbook.nist.gov>>.
- [29] G.A. Parsafar, E.A. Mason, *J. Phys. Chem.* 97 (1993) 9048.
- [30] G.A. Parsafar, F. Kermanpour, B. Najafi, *J. Phys. Chem. B* 103 (1999) 7287.